Acta Biochim Biophys Sin 2013, 45: 391–400 | © The Author 2013. Published by ABBS Editorial Office in association with Oxford University Press on behalf of the Institute of Biochemistry and Cell Biology, Shanghai Institutes for Biological Sciences, Chinese Academy of Sciences. DOI: 10.1093/abbs/gmt030.

Original Article

Hyperhomocysteinemia induces cardiac injury by up-regulation of p53-dependent Noxa and Bax expression through the p53 DNA methylation in ApoE$^{-/-}$ mice

Shengchao Ma[1†], Huiping Zhang[2†], Weiwei Sun[1], HuiHui Gong[1], Yanhua Wang[1], Changjian Ma[1], Ju Wang[1], Chengjian Cao[1], Xiaoling Yang[3], Jue Tian[3], and Yideng Jiang[4*]

[1]Department of Laboratory Medical, Ningxia Medical University, Yinchuan 750004, China
[2]Department of Prenatal Diagnosis Center, General Hospital of Ningxia Medical University, Yinchuan 750004, China
[3]School of basic medical sciences, Ningxia Medical University, Yinchuan 750004, China
[4]Department of Postdoctoral Workstation, General Hospital of Ningxia Medical University, Yinchuan 750004, China
[†]These authors contributed equally to this work.
*Correspondence address. Tel: +86-951-6980998; Fax: +86-951-6980998; E-mail: jydcan@126.com

Hyperhomocysteinemia (HHcy) is a risk factor for cardiovascular disease and has a strong correlation with heart failure. However, the effects of HHcy on cardiac tissue remain less well understood. To elucidate the role of p53-dependent apoptosis in HHcy-induced cardiac injury, we fed ApoE$^{-/-}$ mice with high methionine diet to establish HHcy model. Serum Hcy, cardiac enzymes, and lipids were measured. The protein levels of Noxa, DNMT1, caspases-3/9, and p53 were determined by enzyme-linked immunosorbent assay. Bcl-2 and Bax proteins were detected by immunohistochemistry staining. S-adenosyl methionine and S-adenosyl homocysteine concentrations were determined by high-performance liquid chromatography. The mRNA levels of *p53* and *DNMT1* were analyzed by real-time polymerase chain reaction (PCR) and the methylation levels of p53 were analyzed by nested methylation-specific-PCR. Our data showed that the concentrations of serum Hcy and lipids were increased in Meth group compared with the N-control group, which indicated that the model was established successfully. The expression levels of p53 and Noxa were increased in Meth group, while the methylation status of p53 was hypomethylation. The activities of caspase-3/9 were increased in Meth group compared with the N-control group. In addition, immunohistochemistry staining showed that the expression of Bax was significantly increased in Meth and Meth-F group compared with the N-control group. In summary, HHcy induces cardiac injury by up-regulation of p53-dependent pro-apoptotic related genes *Noxa* and *Bax*, while p53 DNA hypomethylation is a key molecular mechanism in pathological process induced by HHcy.

Keywords hyperhomocysteinemia; cardiac injury; p53; DNA methylation

Received: October 26, 2012 Accepted: March 5, 2013

Introduction

In recent years, many studies have demonstrated that hyperhomocysteinemia (HHcy) is a risk factor for higher mortality and poor left ventricular systolic function in patients following acute myocardial infarction [1]. Numerous mechanisms have been proposed to explain the pathological changes of elevated plasma homocysteine (Hcy) level that is associated with disturbed cardiac substrate metabolism and mitochondrial dysfunction, as well as adverse cardiac remodeling with increased myocardial stiffness [2,3]. However, the direct mechanism responsible for cardiac injury induced by HHcy remains largely unknown.

Cardiac injury is one of the leading causes of morbidity and mortality worldwide. Cardiac apoptosis is evidently followed by cardiac injury, which is accompanied with acute coronary occlusion and ultimately progresses into heart failure [4]. Previous reports have shown that the tumor suppressor p53 plays a critical role in cardiac apoptosis [5]. p35 is an important transcription factor that regulates apoptosis, cell cycle progression, and cellular senescence. Under physiological condition, the expression level of p53 maintains low, but it is elevated when cells are stressed or damaged. p53 is involved in pro-apoptotic and anti-apoptotic activities through transcriptional activation of a large number of target genes, such as *Noxa*, *Bax*, *Bcl-2*, *cytochrome c*, as well as *caspase* genes [6]. Bcl-2 has been reported to regulate an antioxidant pathway at sites of free radical generation, which may be crucial in inhibiting apoptosis [7]. Bax, a member of Bcl-2 family, opposes the protective effects of Bcl-2 and facilitates apoptosis. Importantly, the activity of p53 may increase the expression of Bax and decrease Bcl-2 in cells, promoting apoptosis [8]. On the other hand, Noxa is a member of pro-apoptotic BH3-only subfamily in Bcl-2 family and a p53 downstream

target gene, which is mainly regulated by p53. A previous research has demonstrated that Noxa promotes apoptosis *via* p53-dependent and p53-independent mechanisms, which plays a prominent role in the formation and treatment of tumors [9]. Therefore, it is obvious that *p53* is a key target gene that causes cardiac apoptosis. In our previous study, we found that the mRNA expression of *p53* was decreased in vascular smooth muscle cells treated with Hcy. But whether Hcy can exert similar direct toxic effects in p53-dependent manner in cardiomyocytes is unknown, and the molecular mechanism has not been explored completely.

Hcy is a sulfhydryl-containing amino acid either derived from the metabolic demethylation of methionine or remethylation to methionine, which is subsequently converted to S-adenosyl methionine (SAM) to maintain methyl group supplied for DNA methylation reactions [10,11]. After transfer of methyl groups to the fifth position of the cytosine, SAM is converted to S-adenosyl homocysteine (SAH) [12]. DNA methylation is a major epigenetic factor regulating genome reprogramming, cell differentiation and development, and gene expression, which is catalyzed by a family of DNA methyltransferases (DNMTs) including DNMT1, DNMT3a, and DNMT3b [13]. Increasing evidence suggested that HHcy is associated with DNA methylation. Our previous report showed that Hcy-mediated PPARα/γ hypermethylation is an important mechanism to explain the role of DNA methylation in atherosclerosis. Nevertheless, whether intracellular Hcy accumulation damages cardiac tissue via its influence on DNA methylated patterns have not yet been fully substantiated.

In this study, we investigated the molecular mechanism of p53-dependent apoptosis in HHcy-induced cardiac injury. Furthermore, we aimed to explore the role of p53 DNA methylation and the related genes in cardiac injury induced by HHcy and to find a useful target for the prevention and treatment of diseases caused by HHcy.

Materials and Methods

Animals and treatments

Male ApoE$^{-/-}$ mice (6 weeks old) were provided by the Animal Center of Peking University (Beijing, China). The mice were housed in a climate-controlled room (24°C) and divided randomly into four groups ($n = 12$ each group) and maintained for 15 weeks on the following diets (KeAoXieLi, Beijing, China): (i) normal control group (N-control): fed with regular mouse diet in C57BL/6J mice; (ii) ApoE$^{-/-}$ mice control group (A-control) : fed with regular diet in ApoE$^{-/-}$ mice; (iii) Meth group: fed with regular diet plus 1.7% methionine (wt/wt) in ApoE$^{-/-}$ mice; and (iv) Meth-F group: fed with regular diet plus 1.7% methionine (wt/wt), 0.006% folate and 0.0004% VitB_{12} in ApoE$^{-/-}$ mice. The treatment of the laboratory animals and experimental protocol followed the guidelines of General Hospital of Ningxia Medical University that was approved by the Institutional Authority for Laboratory Animal Care. On the morning of the last day of the diet period, the mice were anesthetized, blood was collected by cardiac puncture and serum was separated by centrifugation (1000 *g* for 10 min at 4°C). Then all the samples were stored at −80°C until further analysis.

Tissue preparation and determination of serum cardiac enzymes, Hcy, and lipids concentrations in ApoE$^{-/-}$ mice

After euthanasia by pentobarbital overdose, the heart was excised and the left ventricle apex was cross-sectioned into specimens (5 mm). Specimens were fixed in 10% formalin (Sigma, St Louis, USA) and embedded in paraffin. Paraffin sections were exhaustively sectioned at 5 μm using a HHQ-2235 Supercut Microtome (Huahai Sciencetific and Educational Instruments, Jinhua, China). The sections were mounted on glass slides, dried on a hotplate at 40°C and incubated at 60°C in an oven for 1 day. Sections were then stained with hematoxylin and eosin. Using a microscope equipped for projection (BX50F4; Olympus, Tokyo, Japan), the sections were projected onto a table top at ×40 magnification. Serum Hcy and cardiac enzyme [aspartate aminotransferase (AST), creatine kinase (CK), MB isoenzyme of creatine kinase (CK-MB), hydroxybutyrate dehydrogenase (HBDH) and lactate dehydrogenase (LDH)] and lipids (total cholesterol, triglyceride, high-density lipoprotein, and low-density lipoprotein) concentrations were measured by ADVIA 2400 Automatic Biochemistry Analyzer (Siemens, Munich, Germany).

Detection of caspase-3/9 activities

Caspase-3/9 activities were measured using caspase activity assay kit (KeyGen, Nanjing, China) according to the manufacturer's instructions. The cardiac tissues (20 mg) were homogenated in lysis buffer and left on ice for 20 min. The lysate was centrifuged at 16,000 *g* at 4°C for 30 min. Supernatants were collected and protein concentrations were measured with a BCA kit (KeyGen). Caspase-3/9 activities were measured by reaction buffer (containing DTT) and caspase substrate peptides Ac-DEVD-pNA and Ac-LEHD-pNA, respectively. The release of p-nitroanilide (pNA) was qualified by determining the absorbance with Tecan Sunrise (Bio-Rad, California, USA) at 405 nm. The absorbance was calculated by the formula [OD_i/OD_0], where OD_0 is the absorbance of control group and OD_i is the absorbance of the other group at the indicated concentration.

Immunohistochemistry staining for Bcl-2 and Bax in the cardiac tissue of ApoE$^{-/-}$ mice

After antigen retrieval and being washed in phosphate-buffer saline (PBS) for 3 min, the sections were incubated with 10% goat serum to block nonspecific binding, and then overlaid with a 150-dilution of anti-Bcl-2 and anti-Bax antibodies (Santa Cruz Biotechnology, Santa Cruz, USA) overnight at 4°C. On the second day, the sections were washed with PBS and incubated at 37°C with the appropriate biotinylated secondary antibody for 1 h, after being washed in PBS. Visualization of antibody binding by DAB staining was performed using the ABC standard kit (Vector Laboratories, California, USA) with DAB/H_2O_2 as substrates according to the manufacturer's instructions. Hematoxylin was used for nuclei counterstaining. Bound antibodies were viewed under an Olympus BX51 microscope. Immunocytochemistry photographs were assessed by densitometry as described previously [14] and analyzed using Image Pro-Plus 6.0 software (Media Cybernetics Company, Silver Spring, USA). The total OD value and area of intracellular brown staining for each section were measured.

Determination of p53, DNMT1, and Noxa by enzyme-linked immunosorbent assay

The cardiac tissues (20 mg) were homogenated in PBS and then centrifuged at 16,000 *g* at 4°C for 3 min. Supernatants were harvested and the concentrations of p53, DNMT1, and Noxa were analyzed by mouse-specific enzyme-linked immunosorbent assay (ELISA) kit (Research & Diagnostics Systems, Minneapolis, USA) according to manufacturer's protocols.

Determination of SAM and SAH concentrations in ApoE$^{-/-}$ mice

The concentrations of SAM and SAH were determined by using high-performance liquid chromatography (HPLC) based on a modification. The SAM and SAH standards (Sigma) were dissolved in 10% perchloric acid ($HClO_4$) water solution at a concentration of 1 mg/ml (1.9 mM) and 10 mg/ml (26 mM), then diluted 40 folds with 10% $HClO_4$ solution to the final concentrations. A total of 10 μl of the mixed SAM and SAH standard solution was injected into HPLC for preparation of standard curve. The cardiac tissues (20 mg) were homogenated and mixed thoroughly in 1 ml of 20% $HClO_4$ solution. Homogenates were placed at 4°C for more than 1 h, and centrifuged at 5000 *g* for 3 min. The supernatants were filtered through 0.22 μm membrane and loaded into a C18 column (4.6 mm × 250 mm I.D., 5 μm particle) (Shimadzu, Tokyo, Japan), then run through a Hitachi L2000 HPLC system (Hitachi, Tokyo, Japan) connected to an ultraviolet detector. Absorption of eluted compounds was monitored at 254 nm. A one-buffer elution system was used: mobile phase contains 0.5 M ammonium formate solution (pH was adjusted to 4.0 with formic acid). Elution of SAM and SAH was achieved at a flow rate of 1.0 ml/min with the mobile phase ammonium formate solution. Chromatograms were recorded by a D-2000 Elite integrator (Hitachi) and its quantification was accomplished by automatic peak area integration. SAM and SAH standards were used to identify the elution peaks. SAM and SAH values of the tissues were calculated according to the standard curve.

Real-time polymerase chain reaction analysis of *DNMT1* and *p53* mRNA expression in cardiac tissue

Total RNA was extracted from 80 mg cardiac tissue in 1 ml Trizol (Invitrogen, Carlsbad, USA). RNA was reversed transcription using Revertid^{TM} first strand cDNA synthesis kit (Thermo Scientific, Glen Burnie, USA) according to the manufacturer's instruction. The cDNA was used for polymerase chain reaction (PCR). Each reaction was performed in triplicate and contained one of the following sets of primers: (i) *DNMT1* forward primer (5′-ACTGCGTCTC GGTCATTC-3′) and reverse primer (5′-GTCTGTGCC TCCCTCCAT-3′); (ii) *p53* forward primer (5′-TACAA GAAGTCACAGCACAT-3′) and reverse primer (5′-GATA GGTCGGCGGTTCAT-3′); and (iii) *GAPDH* forward primer (5′-AGAAGGCTGGGGCTCATTTG-3′) and reverse primer (5′-AGGGGCCATCCACAGTCTTC-3′). The real-time PCR was performed by using a FTC-3000 real-time PCR detection system (FengLing, Shanghai, China). Thermo cycle conditions comprised an initial activation step at 95°C for 5 min, followed by a two-step PCR program of 95°C for 15 s, annealing temperatures at 60°C for 30 s for 45 cycles. An amplification curve was obtained for each real-time PCR. The relative change of *DNMT1* and *p53* mRNA expression was determined by the fold change analysis (*N*), $N = 2^{-\Delta\Delta Ct}$, where $Ct = (Ct_{DNMT1/p53} - Ct_{GAPDH})_{treatment} - (Ct_{DNMT1/p53} - Ct_{GAPDH})_{control}$.

Nested methylation-specific-PCR (nMS-PCR) for p53 methylation assay in the cardiac tissue of ApoE$^{-/-}$ mice

Genomic DNA was isolated from the cardiac tissues using the Wizard® Genomic DNA purification kit (Promega, Madison, USA). An integrated DNA denaturation and bisulfite conversion processes used one-step by EZ DNA Methylation-gold kit (ZYMO, Los Angeles, USA). nMS-PCR consists of two-step PCR amplifications after a standard sodium bisulfite DNA modification. The first step was carried out using an outer primer pair: forward (5′-GG TTAGGTTAGGAGGGAGGTTATT-3′) and reverse (5′-A AAACCCAAAATTCAAACTACAACT-3′). The second step was carried out with the following PCR primers: (i) methylation primer: forward (5′-GGGAACGAGTGTTT

AAAGTTAAGC-3′) and reverse (5′-AAAAAAATACG AAAAACCTATCGAA-3′); (ii) unmethylation primer: forward (5′-GGAATGAGTGTTTAAAGTTAAGTGT-3′) and reverse (5′-AAAAAAATACAAAAAACCTATCAAA-3′). PCR products were purified with an agarose gel DNA fragment recovery kit (Promega) according to the manufacturer's instructions. To reduce mispriming and increase efficiency, touchdown (TD) PCR was used in the amplification. Samples were subjected to 30 cycles in a TD program (94°C for 30 s; 66°C for 30 s and 72°C for 1 min), followed by a 0.5°C decrease of the annealing temperature every cycle). After completion of the TD program, 20 cycles were subsequently run (94°C for 45 s, 51°C for 45 s and 72°C for 45 s), ending with a 5-min extension at 72°C. The PCR products were separated by electrophoresis through a 2% agarose gel containing ethidium bromide. DNA bands were visualized by ultraviolet light. And for simple calculation by the following formula: methylation% = methylation/(methylation+ unmethylation) × 100%.

Statistical analysis

Results are expressed as the mean ± standard error of the mean (SEM). Data were analyzed using one-way analysis of variance and additional analysis using the Student Newman–Keuls test for multiple comparisons within treatment groups or *t*-test for two groups. $P < 0.05$ was considered significant.

Results

Levels of serum total Hcy and lipids in ApoE$^{-/-}$ mice

To confirm whether the HHcy model was established successfully, the levels of serum total (tHcy) were examined. Results showed that serum tHcy was significantly increased in A-control, Meth, and Meth-F groups, with 1.58-, 3.44-, and 1.96-fold increase, respectively, compared with the N-control group, which indicated that a high-methionine diet can induce HHcy in ApoE$^{-/-}$ mice (**Table 1**). However, the level of serum tHcy in Meth-F group was lower than that in Meth group ($P < 0.01$), which indicated that folate and VitB_{12} can modulate the effect caused by a high methionine diet. At the same time, the levels of serum lipids were detected. Results showed that the levels of serum lipids in Meth group were significantly increased compared with those in A-control group ($P < 0.01$). All these data indicated that the animal model was successfully established that would provide a basis for our subsequent experiments.

Effects of Hcy on cardiac enzymes and caspase-3/9 activities

To elucidate the cardiac injury induced by HHcy, the levels of some cardiac enzymes, including AST, CK, CK-MB, HBDH, and LDH in serum, were measured. As shown in **Fig. 1**, all these cardiac enzymes in Meth group have significant changes compared with the N-control group: AST down to 1.60 folds; however CK, LDH, and HBDH up to 1.72, 2.48, and 2.12 folds, respectively, compared with N-control group ($P < 0.05$, $P < 0.01$), which indicated that HHcy might induce the most severe cardiac injury. Compared with the Meth group, CK and CK-MB were decreased by 55.8% and 42.8%, respectively, in the Meth-F group ($P < 0.05$), which suggested that the folate and VitB_{12} relieved cardiac injury caused by HHcy.

The activity of caspase-3 has been shown to be essential in the process of Hcy-induced apoptosis [15], which is activated by an initiator caspase such as caspase-9, with its loss blocking effector caspase activation. These activated caspases cleave many cellular substrates, ultimately leading to apoptosis [16], so we assayed the activities of caspase-3/9. Results showed that the activity of caspase-9 in

Table 1 Serum tHcy and lipid levels in ApoE$^{-/-}$ mice

Group	tHcy (μM)	TC (mM)	TG (mM)	HDL (mM)	LDL (mM)
N-Control	6.50 ± 0.21	2.01 ± 0.10	0.33 ± 0.08	1.25 ± 0.07	0.42 ± 0.01
A-Control	10.25 ± 0.86*	12.81 ± 1.34**	0.81 ± 0.09	0.62 ± 0.06**	0.76 ± 0.09
Meth	22.34 ± 1.55**,##	23.44 ± 1.47**,##	1.98 ± 0.44**,##	0.45 ± 0.03**,#	1.60 ± 0.29**,##
Meth-F	12.71 ± 1.81**,ΔΔ	18.98 ± 0.80**,ΔΔ	1.62 ± 0.25**	0.61 ± 0.02**,Δ	1.05 ± 0.05*,Δ

Values are expressed as the mean ± SEM. $n = 12$.

tHcy, total homocysteine; TC, total cholesterol; TG: triglyceride; HDL: high-density lipoprotein; LDL: low-density lipoprotein.

*$P < 0.05$.

**$P < 0.01$ vs. N-control group.

#$P < 0.05$.

##$P < 0.01$ vs. A-control group.

Δ$P < 0.05$.

ΔΔ$P < 0.01$ vs. Meth group.

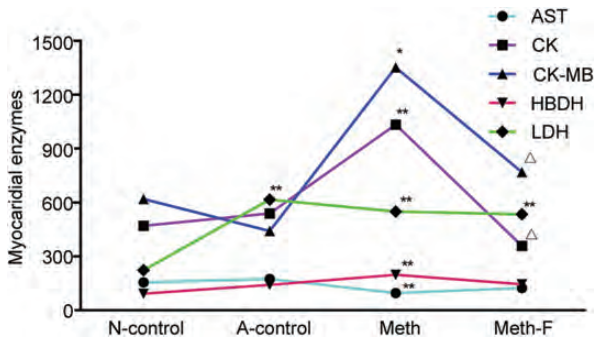

Figure 1 The levels of serum cardiac enzymes after 15 weeks diet treatment of the ApoE$^{-/-}$ mice, the cardiac enzymes (AST, CK, CK-MB, HBDH, and LDH) were measured Data are presented as the mean ± SEM. *$P < 0.05$, **$P < 0.01$ vs. N-control group, $^{\Delta}P < 0.05$ vs. Meth group. $n = 12$.

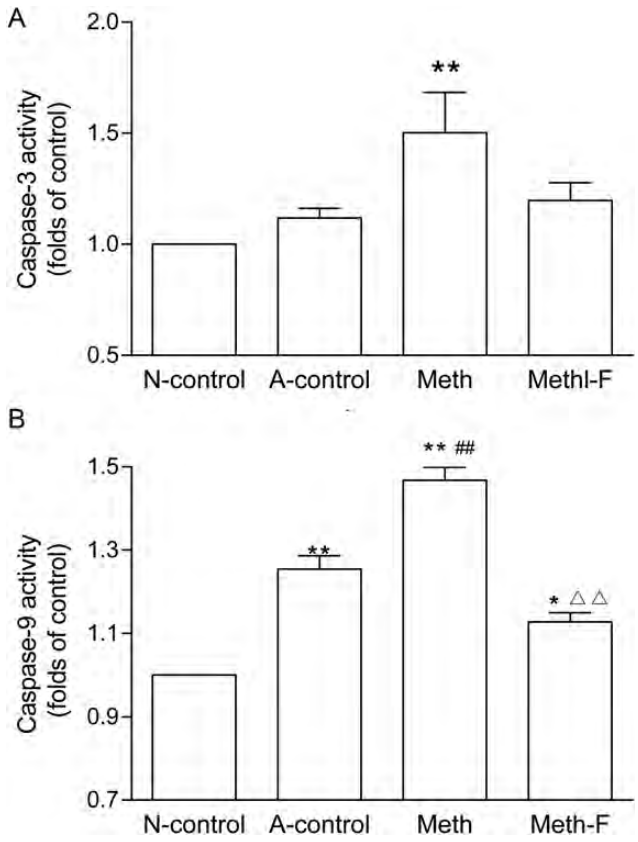

Figure 2 The activities of caspase-3 and -9 in ApoE$^{-/-}$ mice (A) The activity of caspase-3 in ApoE$^{-/-}$ mice. (B) The activity of caspase-9 activity in ApoE$^{-/-}$ mice. Data are presented as the mean ± SEM. *$P < 0.05$, **$P < 0.01$ vs. N-control group. $n = 12$.

experimental groups up to 1.26, 1.47, and 1.13 folds, respectively, compared with N-control group ($P < 0.05$, < 0.01) [**Fig. 2(B)**]. However, the activity of caspase-3 increased by 50.1% in Meth group compared with N-control group ($P < 0.01$); meanwhile, the activities of caspase-3 in the A-control group and the Meth-F group were increased by 12.0% and 20.0% respectively, compared with N-control group [**Fig. 2(A)**]. These findings further confirmed that HHcy can enhance cardiomyocyte apoptosis, and then lead to cardiac injury.

Hcy induced the expression levels of p53, Bcl-2, Bax and Noxa

p53 is the most prominent tumor suppressor, and several key pro-apoptotic genes are regulated by p53, such as *Noxa*, *Bax*, *Bcl-2*, *cytochrome c* and *caspase* genes. To understand whether Hcy regulates p53 *via* Bcl-2 and Bax expressions in cardiac injury, the expression levels of p53, Bcl-2, Bax and Noxa were examined. As shown in **Fig. 3(A,B)**, the intensity of Bcl-2 expression had no obvious change in all groups. In addition, immunohistochemistry staining for Bax of the cardiac tissues from Meth and Meth-F groups indicated that the densitometry was increased significantly compared with the N-control [**Fig. 3(C,D)**; $P < 0.01$)]. On the other hand, compared with N-control group, the Bax/Bcl-2 ratio in Meth group was increased by 1.27 folds [**Fig. 3(E)**; $P < 0.01$] and 1.19 folds compared with A-control group in Meth group [**Fig. 3(E)**; $P < 0.05$]. These findings suggested that HHcy induced apoptosis and might be involved in the regulation of the mitochondrion-mediated apoptosis pathway.

Noxa is a pro-apoptotic BH3-only member of the Bcl-2 family that is up-regulated at a transcriptional level by p53 in response to cellular stresses such as DNA damage or growth factor deprivation [17]. It can interact with anti-apoptotic members of the Bcl-2 family and cause release of cytochrome c into the cytosol, leading to the activation of caspases and induction of apoptosis [18]. Therefore, ELISA was used to measure the expression levels of p53 and Noxa. The expression levels of p53 in Meth and Meth-F groups were much higher than that in the N-control group, up to 1.57 and 1.44 folds, respectively, indicating that HHcy promoted the expression of p53 in ApoE$^{-/-}$ mice. Meanwhile, folate and VitB_{12} alleviated this effect [**Fig. 4(A)**]. The mRNA levels of *p53* in the cardiac tissue were subsequently analyzed [**Fig. 4(B,C)**]. In addition, to assess whether the induction of *Noxa* is essential for p53-dependent apoptosis, we evaluated the expression level of *Noxa*. Our results showed that it was increased in Meth and Meth-F groups, up to 1.25 and 1.20 folds, respectively, compared with N-control group ($P < 0.01$) [**Fig. 4(D)**]. These results suggested that HHcy can induce cardiac injury by up-regulation of p53-dependent pro-apoptotic-related genes *Noxa* and *Bax*, but not anti-apoptotic *Bcl-2*.

The methylation status of p53 and the mechanisms of methylation in ApoE$^{-/-}$ mice

DNA methylation plays a key role in genomic imprinting and CpG islands are found in the promoter region of *p53*,

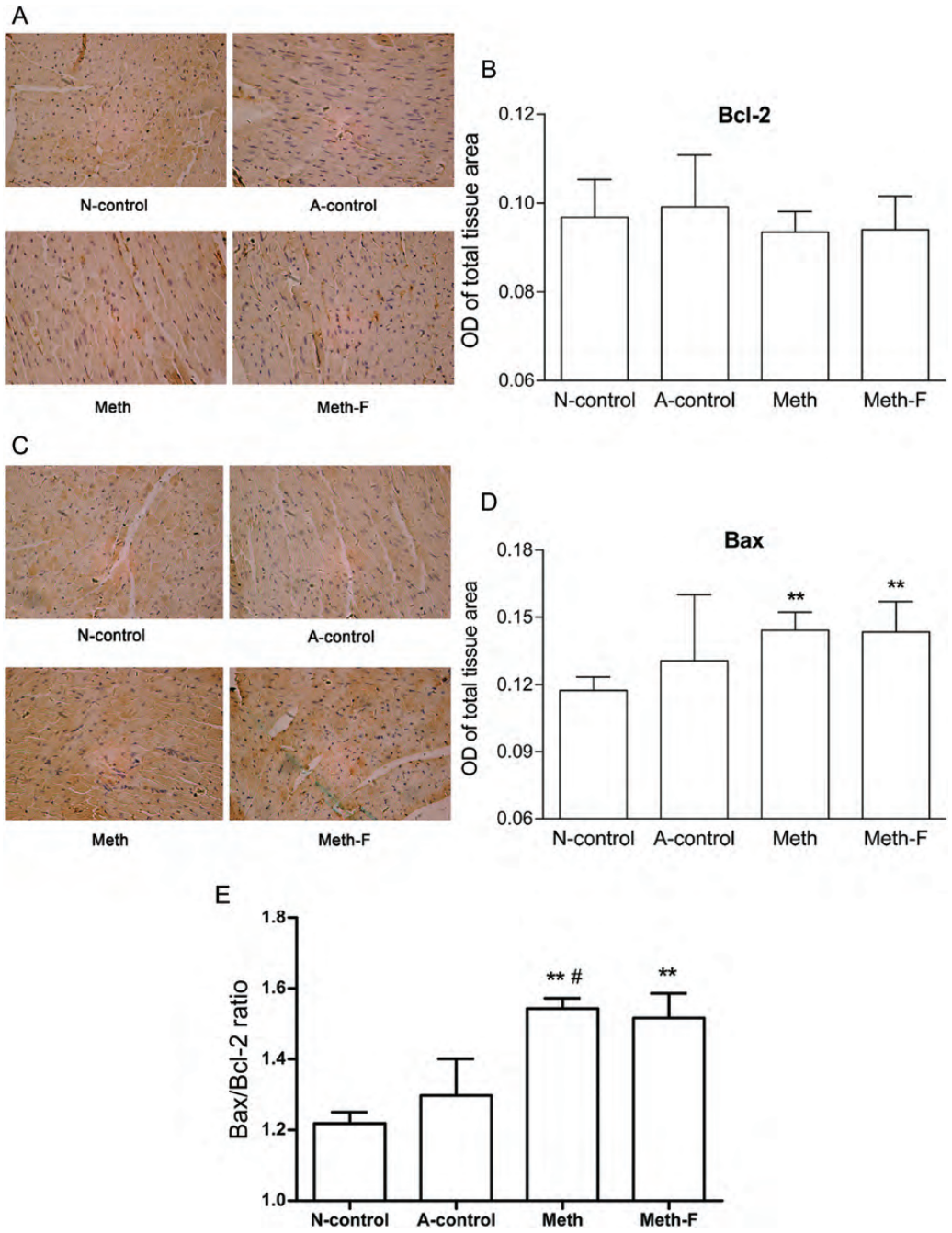

Figure 3 The expression levels of Bcl-2 and Bax in ApoE$^{-/-}$ mice (A) The immuno- histochemistry staining graph of Bcl-2. (B) The expression of Bcl-2. (C) The immunohistochemistry staining graph of Bax in ApoE$^{-/-}$ mice. (D) The expression of Bax in ApoE$^{-/-}$ mice. The cardiac tissues were isolated from ApoE$^{-/-}$ mice, and the tissues were collected and processed for immunohistochemical analysis. Immunohistochemistry showed brown staining in four groups. Immunocytochemistry photographs were assessed by densitometry and analyzed using Image Pro-Plus 6.0 software. The total OD value and area of intracellular brown staining for each section were measured. Pictures depict typical pattern of staining (original magnification: $\times 200$). (E) The ratio of Bax/Bcl-2 in ApoE$^{-/-}$ mice. Values are expressed as the mean $\pm$ SEM. $^{**}P < 0.01$ vs. N-control group. $^{\#}P < 0.05$: Meth vs. A-control. $n = 12$.

so we analyzed the p53 DNA methylation. As depicted in **Fig. 5**, the methylation levels of p53 in A-control group and Meth group significantly increased by 14.30% and 8.32%, respectively ($P < 0.05$, $P < 0.01$), compared with the N-control group, while the methylation levels of p53 in Meth group decreased by 5.21% compared with the A-control group ($P < 0.05$). These data indicated that Hcy inhibited the p53 DNA methylation (**Fig. 5**).

DNMT1 is classically known for its function as a maintenance methyltransferase [19]. To verify the role of DNMT1 in HHcy-induced p53 hypomethylation, the activity of DNMT1 was analyzed by ELISA. The activity of

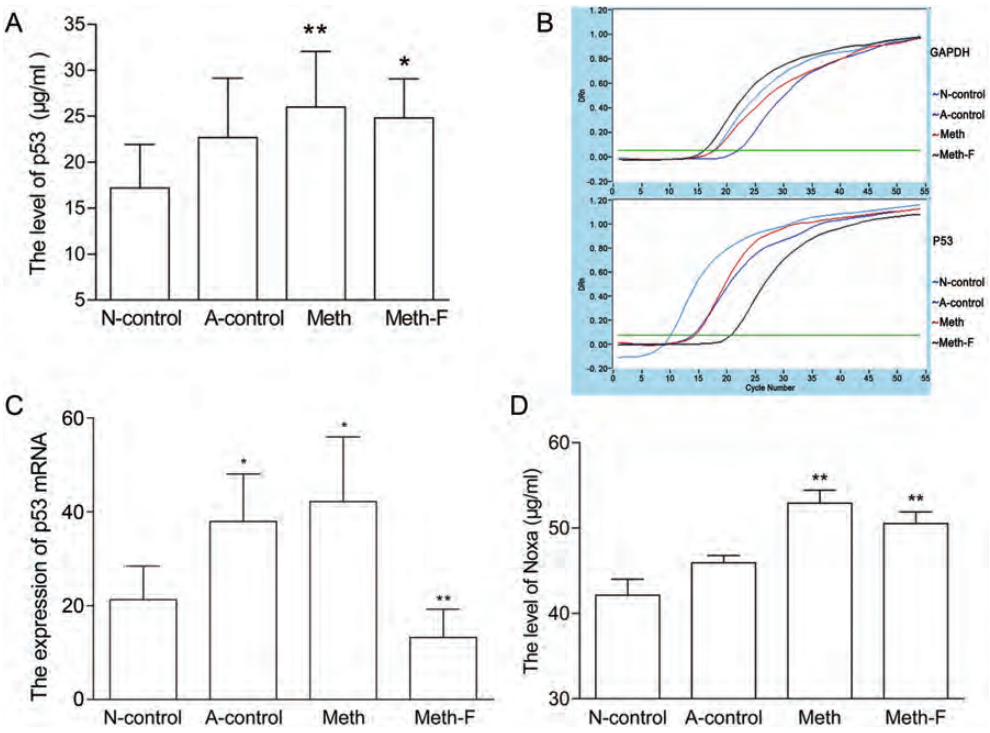

Figure 4 Hcy induced p53 and Noxa expression in ApoE$^{-/-}$ mice (A) The levels of p53 were analyzed by ELISA. (B) The representative graph of *p53* real-time PCR. (C) The expression of *p53* mRNA detected by real-time PCR. (D) The activities of Noxa were analyzed by ELISA. Data are presented as the mean ± SEM. *$P < 0.05$, **$P < 0.01$ vs. N-control group. $n = 12$.

DNMT1 was increased to 14.19%, 15.88%, and 2.11% compared with the N-control group [**Fig. 6(A)**]. These results suggested that DNMT1 played a crucial role in p53 DNA hypomethylation that caused by HHcy.

SAM and SAH are important intermediates in the transmethylation process [20]. To illustrate the mechanism of HHcy-induced p53 DNA hypomethylation in ApoE$^{-/-}$ mice, the concentrations of SAM and SAH were detected by HPLC [**Fig. 6(B,C)**]. The levels of SAM and SAM/SAH ratio increased significantly in A-control group, up to 1.43 and 1.37 folds, respectively ($P < 0.05$, $P < 0.01$), compared with the N-control group. However, the level of SAM in Meth group decreased by 2.51% compared with A-control group ($P < 0.05$). The levels of SAM, SAH, and the ratio of SAM/SAH may act together on the pathogenesis of aberrant DNA methylation.

Discussion

In this study, we aimed to elucidate the molecular mechanism of cardiac injury induced by HHcy and to determine the functional role of p53 DNA methylation. Results indicated that p53 was activated in HHcy-induced cardiac injury. The stimulation of p53 was accompanied with up-regulation of Noxa, the enhanced expression of Bax and caspase-dependent apoptosis in cardiomyocytes, which suggested that Noxa and Bax played dominant roles in HHcy-induced cardiac injury. We further investigated its molecular mechanisms and found that p53 DNA hypomethylation was associated with increased DNMT1 activity and decreased SAM and SAM/SAH ratio in response to cardiac injury induced by HHcy.

First, the ApoE$^{-/-}$ mice has higher success rate of replication HHcy model than normal mice, so we chose ApoE$^{-/-}$ mice to establish the HHcy model to elucidate the molecular mechanism of HHcy-induced cardiac injury. Results showed that serum tHcy was significantly increased 3.44 folds in Meth group compared with N-control group, and a moderate increase of lipids levels in each experimental group, especially in the Meth group. These results are consistent with the report that Hcy can interfere with lipids metabolism [21]. Therefore, results indicated the HHcy model was established successfully.

Second, previous studies have shown that apoptosis has been frequently reported in endothelial cells, contributing to the proatherogenic effects of Hcy [22]. In this study, we examined the expression levels of some cardiac enzymes and apoptosis-related genes. On one hand, the levels of cardiac enzymes were significantly increased in Meth group compared with the N-control group. It has been demonstrated that cardiac enzymes above are widely present in the cytoplasm of cardiomyocytes, and elevation of these enzymes are reliable indicators of cardiac injury [23,24]. On the other hand, it was demonstrated that cell apoptosis was caspase-dependent,

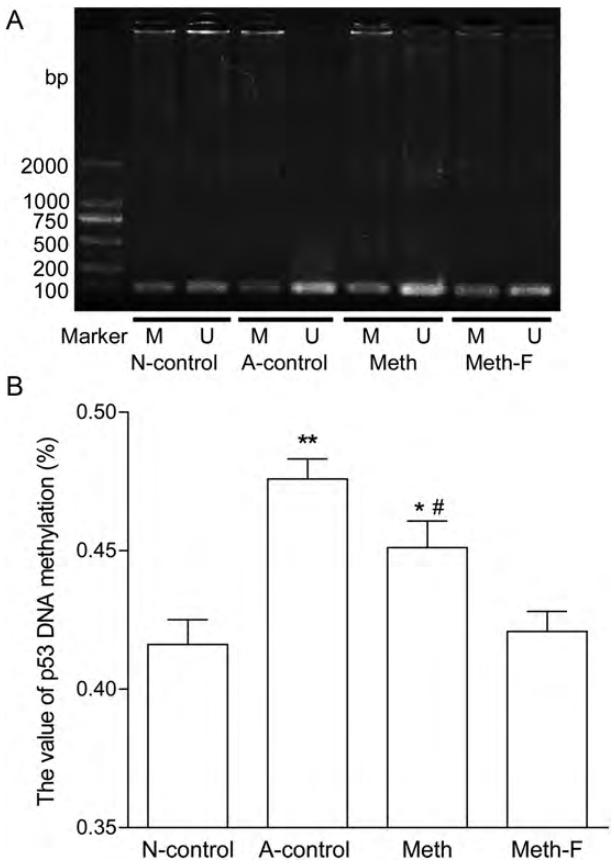

Figure 5 The methylation level of p53 detected by nMS-PCR (A) Photomicrographs and analyses of the p53 DNA methylation levels. (B) Statistical analysis of p53 DNA methylation. M: amplified band by methylation-specific primer. U: amplified band by unmethylation-specific primer. Values are expressed as mean ± SEM. $^{*}P < 0.05$, $^{**}P < 0.01$ vs. N-control group. $^{\#}P < 0.05$: Meth vs. A-control group. $n = 12$.

and was executed mainly by intrinsic mitochondria-dependent pathway [25]. It has been confirmed that the cytochrome c and caspase-9 are the primary signaling molecules in mitochondria pathway. Caspase-3 is the final effector molecule of cell apoptosis, and known as the most athletic ability of apoptosis effector molecule. Activation of caspase-3 depends on the activation of caspase-9, which is regulated by Bcl-2 family. The apoptosis-inducing effect is dependent more on the balance of Bcl-2 and Bax than on Bcl-2 quantity alone [26]. The ratio of Bax and Bcl-2 protein expression is an indicator for apoptosis. We observed a remarkable up-regulation of the expression of Bax protein and a slight decrease of the Bcl-2 protein, leading to an increase of the Bax/Bcl-2 ratio in ApoE$^{-/-}$ mice. Our results showed that the levels of cardiac enzymes and the activities of caspase-9/3 are all significantly increased, suggesting that HHcy leads to cardiac apoptosis.

Third, on the basis of observations *in vitro*, the enhanced expression and activation of p53 may be sufficient to initiate cardiomyocyte apoptosis. p53 up-regulates the transcription of Bax and attenuates the induction of Bcl-2, which facilitates apoptosis [27]. However, our data showed that HHcy induced cardiac apoptosis by promoting the expression of Bax. A previous report suggested that p53 might up-regulate the myocyte renin-angiotensin system, in combination with a decrease the Bcl-2/Bax, leading to cardiomyocyte death [28]. Because of the promoter of Bax containing one perfect and three imperfect consensus binding sites for p53, the activation of p53 may stimulate the *Bax* gene. As a study reported that Hcy increased the expression of p53 and its transactivated gene *Noxa*, leading to cytochrome c release and caspase-9/3 activation in HUVECs [29]. It has also been demonstrated that Hcy induced apoptosis by increasing p53-dependent Noxa expression in mouse endothelial cells [30]. We also found that Hcy significantly increased the expression levels of p53 and Noxa. Therefore, our results suggested that HHcy induced cardiac apoptosis by up-regulation of p53-dependent pro-apoptotic related genes *Noxa* and *Bax* expression, but not anti-apoptotic *Bcl-2*, which provided a new insight for the molecular mechanism in the pathogenesis of HHcy-induced cardiac apoptosis.

Furthermore, to further investigate the mechanisms of p53-dependent up-regulation of Noxa and Bax expressions. Our study revealed that p53 DNA hypomethylation induced by HHcy is a key molecular mechanism. And some researches of DNA hypomethylation unveiled the dominant role of DNMT1 which displayed obvious up-regulation of mRNA and increased activity [31]. Our results showed that the activity of p53 was increased, which was consistent with the survey above. However, the activity of DNMT1 was increased, which contradicted with p53 DNA hypomethylation. It has been reported that DNA methylation inhibits gene expression either by directly interfering with transcription factor binding to DNA [32] or by the recruitment of methyl CpG binding proteins (MBDs), which complex with co-repressor(s) and histone modification enzymes. $MeCP_2$, a member of the MBDs, binds methylated DNA and serves as a transcriptional repressor [33]. It was indicated that p53 DNA hypomethylation might be regulated by $MeCP_2$ and histone acetylation or influenced each other by combinating different factors. These hypotheses are worth to be further studied. Our data showed that Hcy decreased SAM and SAM/SAH ratio in the Meth group. Since SAM is the major methyl group donor, while SAH is a potent inhibitor of cellular transmethylation reaction. A reasonable deduction was that the hypomethylation was a passive process due to the decrease of SAM and SAM/SAH ratio.

Finally, the supplement of folate and $VitB_{12}$ demonstrated mild ameliorative effects against the deteriorative roles of high methionine diet. Hcy remethylation to methionine is an essential metabolism route, which is catalyzed by methionine synthase (MTR) [34]. The MTR requires 5-methyl tetrahydrofolate (5-MTHF) as a methyl donor and

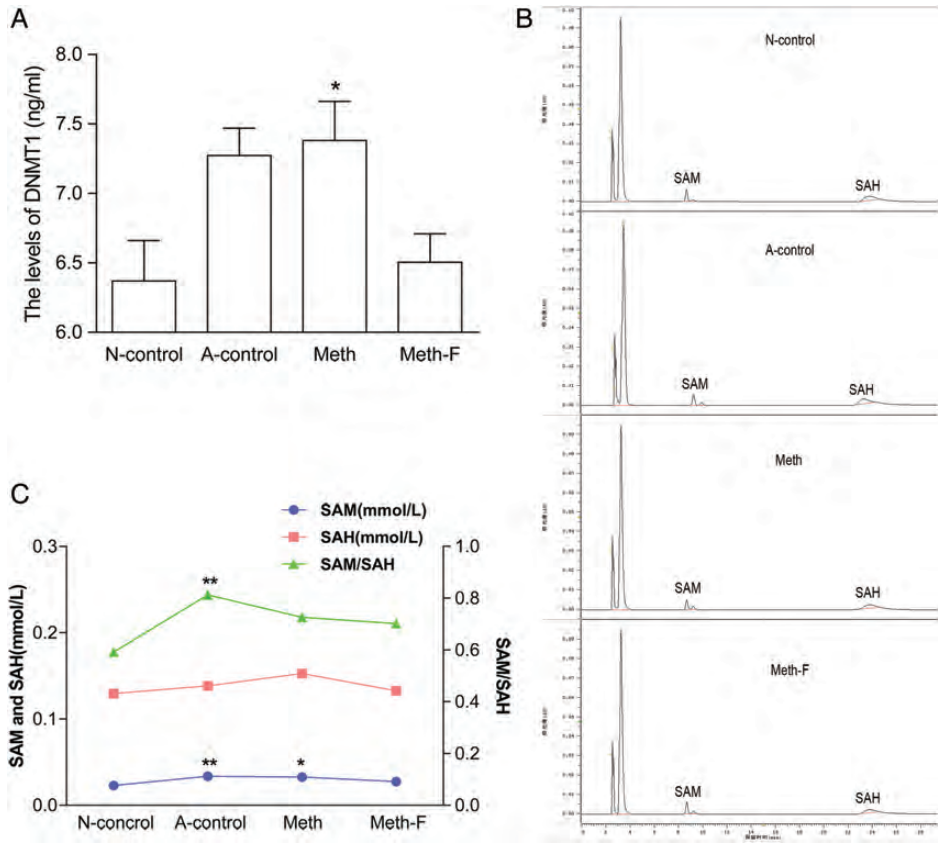

Figure 6 The detection of DNMT1 expression and contents of SAH and SAM (A) Hcy induced DNMT1 expression in cardiac tissues of ApoE$^{-/-}$ mice. (B) The effects of Hcy on SAH, SAM and SAM/SAH ratio in cardiac tissues of ApoE$^{-/-}$ mice. Quantification of SAM, SAH was accomplished by automatic peak area integration. SAM and SAH standards were used to identify the elution peaks, chromatograms were recorded by an integrator. Values are expressed as the mean ± SEM. *$P < 0.05$, **$P < 0.01$ vs. N-control group. $n = 12$.

$VitB_{12}$ as a cofactor. An accumulating body of evidence over the past decades suggested that folate may play a significant modulatory role in the development and prevention of several malignancies. Researchers observed a strong decrease in risk on Hcy-lowering therapy with folate in vascular disease of inborn errors of Hcy metabolism [35]. Therefore, addition of folate and $VitB_{12}$ may influence the metabolism of Hcy, and then disturb the methylation of p53 and the expressions of related genes.

In this study, the data provide new insight for the molecular mechanism by which p53-dependent up-regulation of pro-apoptotic related genes *Noxa* and *Bax* expressions, which play dominant roles in the pathogenesis of HHcy-induced cardiac apoptosis, and then enhanced cardiac injury. We also showed that p53 DNA hypomethylation is a key molecular mechanism in pathological process induced by HHcy. Thus, regulation of DNA methylation may possess therapeutic potential in cardiac injury that is induced by HHcy.

Funding

This work was supported by the grants from the National Natural Science Foundation of China (30960124, 81160044), the New Century Excellent Talents in University (NCET-10-0916), Ningxia Science and Technique Project (20100820), and Ningxia Education, Department Scientific and Technological Project ([2012]17).

References

1 Beard RS Jr and Bearden SE. Vascular complications of cystathionine β-synthase deficiency: future directions for homocysteine-to-hydrogen sulfide research. Am J Physiol Heart Circ Physiol 2011, 300: H13–H26.
2 Maldonado C, Soni CV, Todnem ND, Pushpakumar S, Rosenberger D, Givvimani S and Villafane J, *et al*. Hyperhomocysteinemia and sudden cardiac death: potential arrhythmogenic mechanisms. Curr Vasc Pharmacol 2010, 8: 64–74.
3 Moshal KS, Metreveli N, Frank I and Tyagi SC. Mitochondrial MMP activation, dysfunction and arrhythmogenesis in hyperhomocysteinemia. Curr Vasc Pharmacol 2008, 6: 84–92.
4 Misra A, Haudek SB, Knuefermann P, Vallejo JG, Chen ZJ, Michael LH and Sivasubramanian N, *et al*. Nuclear factor-κB protects the adult cardiac myocyte against ischemia-induced apoptosis in a murine model of acute myocardial infarction. Circulation 2003, 108: 3075–3078.
5 Feridooni T, Hotchkiss A, Remley-Carr S, Saga Y and Pasumarthi KB. Cardiomyocyte specific ablation of p53 is not sufficient to block

doxorubicin induced cardiac fibrosis and associated cytoskeletal changes. PLoS One 2011, 6: e22801.
6 Shankar S and Srivastava RK. Involvement of Bcl-2 family members, phosphatidylinositol 3′-kinase/AKT and mitochondrial p53 in curcumin (diferulolylmethane)-induced apoptosis in prostate cancer. Int J Oncol 2007, 30: 905–918.
7 Halasova E, Adamkov M, Matakova T, Vybohova D, Antosova M, Janickova M, Singliar A and Dobrota D, *et al*. Expression of Ki-67, Bcl-2, survivin and p53 proteins in patients with pulmonary carcinoma. Adv Exp Med Biol 2013, 756: 15–21.
8 Gryko M, Pryczynicz A, Guzińska-Ustymowicz K, Kamocki Z, Zaręba K, Kemona A and Kędra B. Immunohistochemical assessment of apoptosis-associated proteins: p53, Bcl-xL, Bax and Bak in gastric cancer cells in correlation with clinical and pathomorphological factors. Adv Med Sci 2012, 71: 77–83.
9 Schuler M, Maurer U, Goldstein JC, Breitenbücher F, Hoffarth S, Waterhouse NJ and Green DR. p53 triggers apoptosis in oncogene-expressing fibroblasts by the induction of Noxa and mitochondrial Bax translocation. Cell Death Differ 2003, 10: 451–460.
10 Chen NC, Yang F, Capecci LM, Gu Z, Schafer AI, Durante W, Yang XF and Wang H. Regulation of homocysteine metabolism and methylation in human and mouse tissues. FASEB J 2010, 24: 2804–2817.
11 Anderson OS, Sant KE and Dolinoy DC. Nutrition and epigenetics: an interplay of dietary methyl donors, one-carbon metabolism and DNA methylation. J Nutr Biochem 2012, 23: 853–859.
12 Jiang Y, Zhang H, Sun T, Wang J, Sun W, Gong H and Yang B, *et al*. The comprehensive effects of hyperlipidemia and hyperhomocysteinemia on pathogenesis of atherosclerosis and DNA hypomethylation in $ApoE^{-/-}$ mice. Acta Biochim Biophys Sin 2012, 44: 866–875.
13 Arand J, Spieler D, Karius T, Branco MR, Meilinger D, Meissner A and Jenuwein T, *et al*. *In vivo* control of CpG and non-CpG DNA methylation by DNA methyltransferases. PLoS Genet 2012, 8: e1002750.
14 Esposito E, Rinaldi B, Mazzon E, Donniacuo M, Impellizzeri D, Paterniti I and Capuano A, *et al*. Anti-inflammatory effect of simvastatin in an experimental model of spinal cord trauma: involvement of PPAR-α. J Neuroinflammation 2012, 9: 81.
15 Wang X, Cui L, Joseph J, Jiang B, Pimental D, Handy DE and Liao R, *et al*. Homocysteine induces cardiomyocyte dysfunction and apoptosis through p38 MAPK-mediated increase in oxidant stress. J Mol Cell Cardiol 2012, 52: 753–760.
16 Hsiao WT, Tsai MD, Jow GM, Tien LT and Lee YJ. Involvement of Smac, p53, and caspase pathways in induction of apoptosis by gossypol in human retinoblastoma cells. Mol Vis 2012, 18: 2033–2042.
17 Rooswinkel RW, van de Kooij B, Verheij M and Borst J. Bcl-2 is a better ABT-737 target than Bcl-xL or Bcl-w and only Noxa overcomes resistance mediated by Mcl-1, Bfl-1, or Bcl-B. Cell Death Dis 2012, 3: e366.
18 Jullig M, Zhang WV, Ferreira A and Stott NS. MG132 induced apoptosis is associated with p53-independent induction of pro-apoptotic Noxa and transcriptional activity of beta-catenin. Apoptosis 2006, 11: 627–641.
19 Clements EG, Mohammad HP, Leadem BR, Easwaran H, Cai Y, Van Neste L and Baylin SB. DNMT1 modulates gene expression without its catalytic activity partially through its interactions with histone-modifying enzymes. Nucleic Acids Res 2012, 40: 4334–4346.
20 Lin HC, Hsieh HM, Chen YH and Hu ML. S-Adenosylhomocysteine increases beta-amyloid formation in BV-2 microglial cells by increased expressions of beta-amyloid precursor protein and presenilin 1 and by hypomethylation of these gene promoters. Neurotoxicology 2009, 30: 622–627.
21 Zhang J, Handy DE, Wang Y, Bouchard G, Selhub J, Loscalzo J and Carey MC. Hyper- homocysteinemia from trimethylation of hepatic phosphatidylethanolamine during cholesterol cho- lelithogenesis in inbred mice. Hepatology 2011, 54: 697–706.
22 Sipkens JA, Hahn NE, Blom HJ, Lougheed SM, Stehouwer CD, Rauwerda JA and Krijnen PA, *et al*. S-Adenosylhomocysteine induces apoptosis and phosphatidylserine exposure in endothelial cells independent of homocysteine. Atherosclerosis 2012, 221: 48–54.
23 Henning RJ, Dennis S, Sawmiller D, Hunter L, Sanberg P and Miller L. Human umbilical cord blood mononuclear cells activate the survival protein Akt in cardiac myocytes and endothelial cells that limits apoptosis and necrosis during hypoxia. Transl Res 2012, 159: 497–506.
24 Li YC, Ge LS, Yang PL, Tang JF, Lin JF, Chen P and Guan XQ. Carvedilol treatment ameliorates acute coxsackievirus B3-induced myocarditis associated with oxidative stress reduction. Eur J Pharmacol 2010, 640: 112–116.
25 Silva-Platas C, García N, Fernandez-Sada E, Davila D, Hernandez-Brenes C, Rodriguez D and García-Rivas G. Cardiotoxicity of acetogenins from *Persea americana* occurs through the mitochondrial permeability transition pore and caspase-dependent apoptosis pathways. J Bioenerg Biomembr 2012, 44: 461–471.
26 Ghobrial IM, Witzig TE and Adjei AA. Targeting apoptosis pathways in cancer therapy. CA Cancer J Clin 2005, 55: 178–194.
27 Qiao S, Cabello CM, Lamore SD, Lesson JL and Wondrak GT. D-Penicillamine targets metastatic melanoma cells with induction of the unfolded protein response (UPR) and Noxa (PMAIP1)-dependent mitochondrial apoptosis. Apoptosis 2012, 17: 1079–1094.
28 Liu P, Xu B, Cavalieri TA and Hock CE. Inhibition of p53 by pifithrin-alpha reduces myocyte apoptosis and leukocyte transmigration in aged rat hearts following 24 hours of reperfusion. Shock 2008, 5: 545–551.
29 Lee SJ, Kim KM, Namkoong S, Kim CK, Kang YC, Lee H, Ha KS and Han JA, *et al*. Nitric oxide inhibition of homocysteine-induced human endothelial cell apoptosis by down-regulation of p53-dependent Noxa expression through the formation of S-nitrosohomocysteine. J Biol Chem 2005, 280: 5781–5788.
30 Stegh AH and DePinho RA. Beyond effector caspase inhibition: Bcl2L12 neutralizes p53 signaling in glioblastoma. Cell Cycle 2011, 10: 33–38.
31 Kovacheva VP, Mellott TJ, Davison JM, Wagner N, Lopez-Coviella I, Schnitzler AC and Blusztajn JK. Gestational choline deficiency causes global and Igf2 gene DNA hypermethylation by up-regulation of Dnmt1 expression. J Biol Chem 2007, 282: 31777–31788.
32 Tian K, Wang Y, Huang Y, Sun B, Li Y and Xu H. Methylation of WTH3, a possible drug resistant gene, inhibits p53 regulated expression. BMC Cancer 2008, 8: 327.
33 Setoguchi H, Namihira M, Kohyama J, Asano H, Sanosaka T and Nakashima K. Methyl-CpG binding proteins are involved in restricting differentiation plasticity in neurons. J Neurosci Res 2006, 84: 969–979.
34 Sukla KK and Raman R. Association of MTHFR and RFC1 gene polymorphism with hyper- homocysteinemia and its modulation by vitamin B12 and folic acid in an Indian population. Eur J Clin Nutr 2012, 66: 111–118.
35 Bhargava S, Ali A, Bhargava EK, Manocha A, Kankra M, Das S and Mohan Srivastava L. Lowering homocysteine and modifying nutritional status with folic acid and vitamin B12 in Indian patients of vascular disease. J Clin Biochem Nutr 2012, 50: 222–226.